



Aortic wall shear stress in bicuspid aortic valve disease—10-year follow-up

Michael Hanigk¹, Elisabeth Burgstaller¹, Heiner Latus¹, Nerejda Shehu¹, Judith Zimmermann², Stefan Martinoff³, Anja Hennemuth^{4,5}, Peter Ewert¹, Heiko Stern¹, Christian Meierhofer¹

¹Congenital Heart Disease and Pediatric Cardiology, German Heart Center Munich, Technical University of Munich, Munich, Germany;

²Department of Computer Science, Technical University of Munich, Munich, Germany; ³Radiology, German Heart Center Munich, Technical University of Munich, Munich, Germany; ⁴Institute for Computational and Imaging Science in Cardiovascular Medicine, Charité Universitätsmedizin, Berlin, Germany; ⁵Fraunhofer MEVIS Institute for Digital Medicine, Bremen, Germany

Contributions: (I) Conception and design: P Ewert, C Meierhofer, H Stern, M Hanigk; (II) Administrative support: P Ewert, C Meierhofer, M Hanigk, J Zimmermann, S Martinoff, A Hennemuth; (III) Provision of study materials or patients: M Hanigk, E Burgstaller, H Latus; (IV) Collection and assembly of data: C Meierhofer, M Hanigk, E Burgstaller, N Shehu; (V) Data analysis and interpretation: M Hanigk, E Burgstaller, C Meierhofer, H Stern; (VI) Manuscript writing: All authors; (VII) Final approval of manuscript: All authors.

Correspondence to: Michael Hanigk. Congenital Heart Disease and Pediatric Cardiology, German Heart Center Munich, Technical University of Munich, Munich, Germany. Email: Michael.Hanigk@t-online.de.

Background: Bicuspid aortic valve (BAV) disease leads to deviant helical flow patterns especially in the mid-ascending aorta (AAo), potentially causing wall alterations such as aortic dilation and dissection. Among others, wall shear stress (WSS) could contribute to the prediction of long-term outcome of patients with BAV. 4D flow in cardiovascular magnetic resonance (CMR) has been established as a valid method for flow visualization and WSS estimation. The aim of this study is to reevaluate flow patterns and WSS in patients with BAV 10 years after the initial evaluation.

Methods: Fifteen patients (median age 34.0 years) with BAV were re-evaluated 10 years after the initial study from 2008/2009 using 4D flow by CMR. Our particular patient cohort met the same inclusion criteria as in 2008/2009, all without enlargement of the aorta or valvular impairment at that time. Flow patterns, aortic diameters, WSS and distensibility were calculated in different aortic regions of interest (ROI) with dedicated software tools.

Results: Indexed aortic diameters in the descending aorta (DAo), but especially in the AAo did not change in the 10-year period. Median difference 0.05 cm/m² (95% CI: 0.01 to 0.22; P=0.06) for AAo and median difference -0.08 cm/m² (95% CI: -0.12 to 0.01; P=0.07) for DAo. WSS values were lower in 2018/2019 at all measured levels. Aortic distensibility decreased by median 25.6% in the AAo, while stiffness increased concordantly (median +23.6%).

Conclusions: After a ten years' follow-up of patients with isolated BAV disease, indexed aortic diameters did not change in this patient cohort. WSS was lower compared to values generated 10 years earlier. Possibly a drop of WSS in BAV could serve as a marker for a benign long-term course and implementation of more conservative treatment strategies.

Keywords: Bicuspid aortic valve (BAV); wall shear stress (WSS); cardiovascular magnetic resonance (CMR); 4D flow; aortic diameter

Submitted Sep 21, 2022. Accepted for publication Dec 19, 2022. Published online Feb 10, 2023.

doi: 10.21037/cdt-22-477

View this article at: <https://dx.doi.org/10.21037/cdt-22-477>

Introduction

Bicuspid aortic valve (BAV) disease is the most prevalent congenital heart defect, affecting 0.77% to 2% of the general population (1,2). It describes the fusion of two aortic cusps during valvulogenesis leading to an aortic valve consisting of two instead of three leaflets (3). The fusion of the right and left coronary cusp is the most common morphotype (RL-type) followed by RN-type (fusion of the right and noncoronary cusp) and LN-type (fusion of the left and noncoronary cusp) (4). Frequent complications of this malformation are valvular dysfunction, aortic stenosis (AS) as well as aortic regurgitation (AR) (5) and changes in hemodynamics, leading to complex helical flow patterns (6). Clinically relevant wall alterations may occur, especially in the mid-ascending aorta (AAo), such as dilation, aneurysm formation and dissection (7,8). However, the still unknown origin of these pathologies led to two conflicting theories: the genetic theory is based on a connective tissue disorder named “Erdheim’s cystic medial necrosis” (9) which leads to inborn wall weakness, also explaining the association of BAV with further congenital vascular defects, such as coarctation of the aorta (CoA) or patent ductus arteriosus (1). In contrast, the hemodynamic theory describes a BAV, which in itself is causing flow alterations, which affect the vessel wall, and leads to the development of an aortopathy (10).

Besides aortic diameter, several parameters like wall

shear stress (WSS), aortic distensibility, aortic stiffness and flow displacement were established in recent years for quantification of disease severity and prediction of outcome (11,12). For assessment of these parameters, a combination of non-invasive techniques such as echocardiography (13) and cardiovascular magnetic resonance (CMR) is required. Based on CMR, 4D flow has been established as a valid imaging modality offering the possibility for direct, *in vivo* evaluation of vascular anatomy and cardiac function (14,15). It is applied for flow visualization and WSS estimation (16,17). Due to the gap in longitudinal studies in BAV disease, the aim of this study was to evaluate the diagnostic value of hemodynamic parameters such as flow patterns, distensibility and WSS in BAV but without further cardiovascular disease collecting ten-year follow-up data in the same patient cohort as in 2008/2009 using 4D flow CMR. We present the following article in accordance with the TREND reporting checklist (available at <https://cdt.amegroups.com/article/view/10.21037/cdt-22-477/rc>).

Methods

Study population

A specific patient cohort consisting of fifteen patients with congenital BAV previously evaluated in 2008/2009 were included for reevaluation, performed between October 2018 and September 2019 at a third level cardiac center. The patients were all contacted for this follow-up study. Among this patient group we could also reevaluate a child which was only aged 10 years at that time. In 2008/2009 originally 18 patients with BAV were included, 3 patients (17%) were lost during follow-up due to non-availability of contact data. Before CMR, all subjects underwent clinical examination including physical examination, 12-lead electrocardiography (ECG) and echocardiographic survey of valvular function. Exclusion criteria were equal as in 2008/2009: congenital heart disease other than BAV, aortic dissection, previous myocardial infarction or cardiovascular surgery, connective tissue disorders, hypertension, maximal flow velocity through the aortic valve (V_{max}) of >2.9 m/s and contraindications for CMR imaging. All patients met the inclusion criteria. Patients with moderate or severe aortic valve stenosis or regurgitation were excluded from the initial study. The study was approved by the ethics committee of the Technical University of Munich (No. 29/18S) and all patients gave written informed consent. No participant received financial support. The trial was

Highlight box

Key findings

- After a ten years' follow-up of patients with isolated BAV disease, WSS decreased whilst indexed aortic diameters did not change in this patient cohort.

What is known and what is new?

- BAV disease may lead to aortic dilation, complex helical flow patterns and increased WSS, especially in the mid-ascending aorta.
- 4D flow CMR has been established as a valid imaging modality for flow visualization and WSS estimation.
- WSS reduction might be explained by slight alterations in hemodynamic flow patterns by the aging aorta as distensibility decreased and stiffness index increased both more than 20% after ten years.

What is the implication, and what should change now?

- Possibly a drop of WSS in BAV could serve as a marker for a benign long-term course and implementation of more conservative treatment strategies.

conducted in accordance with the Declaration of Helsinki (as revised in 2013).

CMR

All CMR scans in 2008/2009 and 2018/2019 were performed on the same 1.5 Tesla MRI system (MAGNETOM Avanto[®], software version VD13, Siemens Healthineers, Erlangen, Germany) with a 12-channel body-coil. Re-assessment of aortic valve morphotype and measurement of aortic diameters and planimetric area for distensibility calculation were performed using an ECG-gated time-resolved (2D CINE) steady state free precession (SSFP) sequence over multiple cardiac timeframes during breath hold (slice thickness 6 mm, acquisition matrix 192×192, 25 phases/cardiac cycle). Measurements of aortic diameter and planimetric area were performed in double-oblique, cross-sectional orientation to the aortic root axis by choosing adequate slices representing the maximal aortic diameter at peak systole and end-diastole. Further, aortic blood flow patterns were evaluated using a time-resolved three-dimensional (3D) phase-contrast (PC) sequence with three-directional velocity encoding (4D flow CMR) with prospective gating. A sagittal oblique plane orientation for image acquisition provides 3D volumetric coverage of the entire aorta [from left ventricular outflow tract to the thoracic descending aorta (DAo)]. ECG-synchronization and respiratory navigator-gating were performed. Prospective gating was used due to sequence architecture, since same scanner and the same sequence parameters were set as in the initial study in 2008/2009. No contrast agent was used. Measurement parameters were: isotropic voxel size with a spatial resolution of 2.5×2.5×2.5 mm³, TE 2.44 ms, TR 39.2 ms, FOV 240×320 mm, FOV phase 75%, velocity encoding V_x, V_y, V_z 200–320 cm/s, flip angle 8°, band width 440 Hz/pixel. Image acquisition is displayed in *Figure 1*.

Aortic valve morphotype

Aortic valve morphotype was classified as previously described by Schaefer *et al.*: BAV type 1 describing the congenital fusion of the right and left coronary cusp, BAV type 2 as fusion of the right and noncoronary cusp and BAV

type 3 as fusion of the left and noncoronary cusp (4).

Calculation of distensibility and stiffness index

By using Microsoft Excel software tool (Microsoft Corporation, 2018, Redmond, WA, USA) calculation of distensibility according to a previously described formula was performed:

$$\text{Distensibility} = \frac{A_{\min} - A_{\max}}{(A_{\min} \times [P_{\text{sys}} - P_{\text{dia}}])} 10^{-3} \text{ mmHg}^{-1} \quad [1]$$

where A_{\max} = maximal systolic area (mm²), A_{\min} = minimal diastolic area (mm²), P_{sys} = systolic blood pressure (mmHg) and P_{dia} = diastolic blood pressure (mmHg) (18). Aortic stiffness index (SI) was calculated according to Nistri *et al.*:

$$\text{SI} = \frac{\ln(P_{\text{sys}} - P_{\text{dia}})}{(D_{\max} - D_{\min})/D_{\min}} \quad [2]$$

with D_{\max} describing the maximal systolic aortic diameter and D_{\min} describing the minimal diastolic aortic diameter (19).

Data preprocessing

The generated 4D flow data sets were imported in DICOM format to the current software MEVISFlow (MEVISFlow; Fraunhofer Institute for Digital Medicine, software version 11.4, Bremen, Germany) for further editing. Data sets from 2008/2009, previously analyzed with EnSight[®] software package (EnSight[®]; CEI, Apex, NC, USA) and software tool based on Matlab (The MathWorks, Natick, MA, USA), were also reevaluated by software MEVISFlow using the same parameter settings. Vascular enhancement and suppression of background signal was performed applying noise filtering, eddy-current correction and anti-aliasing as presented by Walker *et al.* (20). After pre-processing, the squared sum of the 3D-PC images provided a time-averaged 3D phase-contrast MR angiography (PC-MRA) for watershed-based 3D segmentation of the complete thoracic aorta, also performed with MEVISFlow. By adjusting the threshold at eddy-current correction (optimum 0.023±0.003), manual correction of 3D segmentations could be reduced to a minimum. The workflow of data

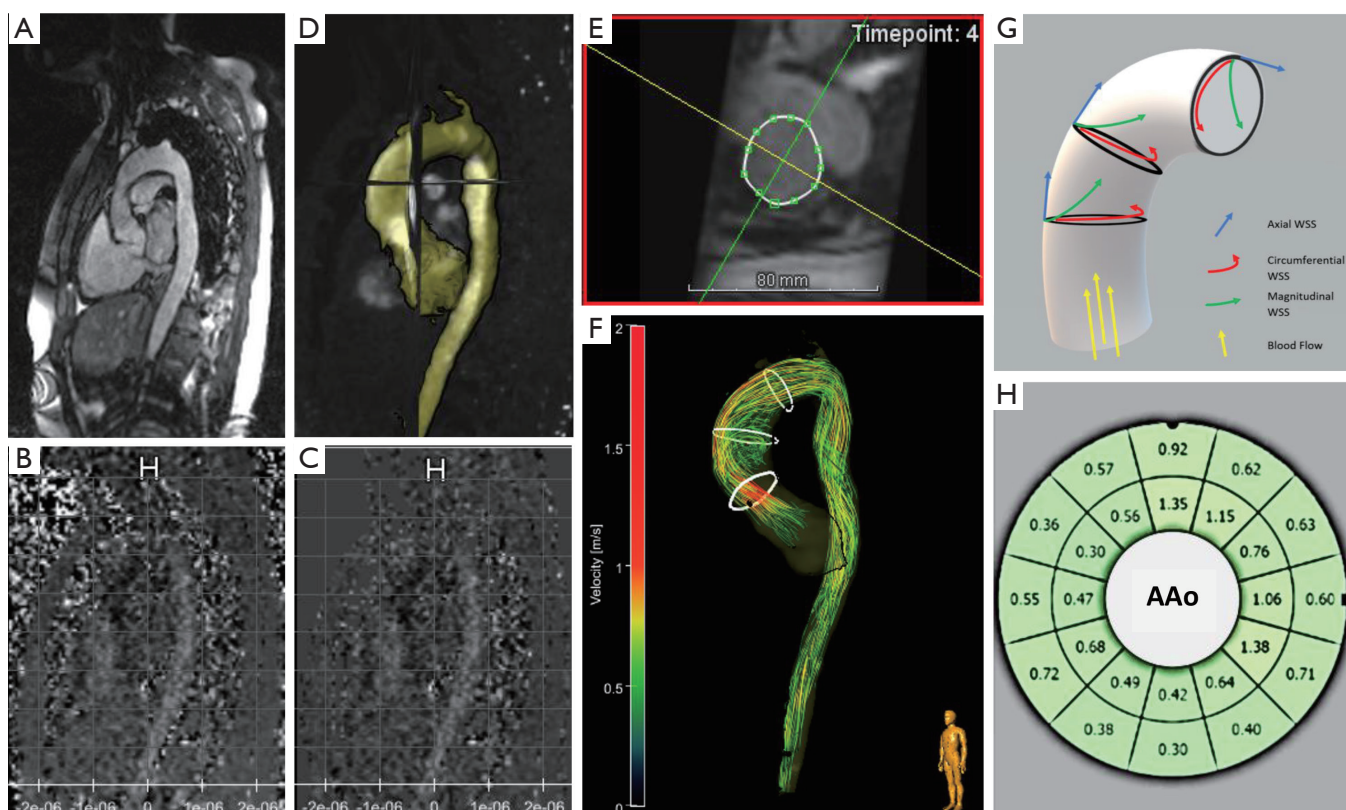


Figure 1 Workflow of 4D flow CMR data, post-processing and WSS estimation. (A) Magnitude image; (B) phase-contrast image; (C) phase-contrast image after applying noise filtering, eddy-current correction and anti-aliasing; (D) 3D segmentation of the complete thoracic aorta; (E) manual contouring of the aortic vessel wall in peak systole defines ROI; (F) visualization of flow patterns using pathline tracing, different ROIs; (G) depiction of axial, circumferential and magnitudinal WSS, curved vectors for better visualization are used, by definition true vectors are straight in orientation; (H) axial WSS values measured in the mid ascending aorta; inner circle: WSS values for specific time-point, outer circle: mean axial WSS including all time-points. Preprocessing, segmentation and WSS estimation was performed using MEVISFlow. AAo, (mid-) ascending aorta; CMR, cardiovascular magnetic resonance; WSS, wall shear stress; ROI, region of interest.

preprocessing is pictured in *Figure 1*.

Flow visualization and WSS estimation

By manually contouring the aortic vessel wall on reformatted cross-sectional magnitude image planes at a single temporal frame in systolic phase, we defined our regions of interest (ROI), displaying important anatomical landmarks (mid-ascending aorta at the level of bifurcation of the main pulmonary artery (MPA level) and at the level just before the branching of the brachiocephalic trunk (BCT level) (*Figure 1*). An automated algorithm further propagated the contour to all other temporal frames, but in a few cases manual correction was necessary to account for motion of the aorta and the most precise vessel lumen

boundary definition as possible (21). 4D flow visualization in the mid-ascending aorta was performed using pathline tracing (22) (*Figure 1*). Flow was classified according to a grading scale previously described by Meierhofer *et al.*, where Grade 0 was defined as linear flow and Grade 1–3 as helical flow (Grade 1: $<180^\circ$, Grade 2: $180\text{--}360^\circ$ and Grade 3: $>360^\circ$) (6). WSS was calculated by separation of blood flow forces acting on the vessel wall into three vectors: axial WSS (WSS_{axial}) – parallel to flow direction; circumferential WSS (WSS_{circ}) – in-plane, and magnitudinal WSS (WSS_{mag}) as resulting net vector represents the entire aortic WSS (23) (*Figure 1*). WSS values were merged over a complete cardiac cycle for each vessel wall segment (*Figure 1*). CMR was operated by experienced investigators (MC, HM, BE and SN). Flow visualization and WSS

estimation was performed by two investigators (HM and BE) both blinded to the findings in 2008/2009 and with more than 2 years of experience in post-processing.

Statistical analysis

Statistical analysis was performed using GraphPad Prism 9.02 statistical software. Data are presented as median and total range. Differences were analyzed using the Wilcoxon signed-rank test. Intra- and inter-observer variability concerning WSS were evaluated using Bland-Altman analysis of matched pairs analyzed by one investigator and two investigators, respectively. Correlation analyses were displayed by Spearman correlation coefficient r .

Results

Study population

The 10-year follow-up reevaluation (median follow-up 9.8 years, range 9.5 to 10.7 years) was successfully completed in fifteen asymptomatic patients (8 males; 53%), median age 34 years (range, 19.8 to 54.3 years), no one had to be excluded. Three patients of the original cohort of 18 patients (17%) were lost to follow-up due to non-availability of contact data. No adverse events or unintended effects occurred during the study. The echocardiographic survey revealed no pronounced valvular dysfunction. The velocity through the aortic valve was median 1.9 m/s (range 0.9 to 2.7 m/s). The regurgitation fraction was median 2.5% (range 0 to 13%). Eleven patients (73%) were identified as BAV type 1, the remaining 4 patients as BAV type 2, confirming the morphotypes of the aortic valve as evaluated in 2008/2009. The statistical analysis demonstrated good evidence of an important difference comparing 2008/2009 values with 2018/2019: weight (median difference 3 kg; range -3 to 25 kg; 95% CI: 1.9 to 9.7; $P=0.005$), body mass index (BMI) (median difference 1.63 kg/m²; range -1.91 to 5.73 kg/m²; 95% CI: 0.4 to 2.8; $P=0.02$), body surface area (BSA) (median difference 0.04 m²; range -0.04 to 0.49 m²; 95% CI: 0.02 to 0.2; $P=0.004$), diastolic blood pressure (median difference 2.5 mmHg; range -11 to 15 mmHg; 95% CI: 0.3 to 5.0; $P=0.04$), velocity through the aortic valve (median difference 0.3 m/s; range -1.4 to 0.8 m/s; 95% CI: -5.0 to 52.8; $P=0.03$) and absolute aortic diameter for AAo (median difference 0.3 cm; range -0.02 to 0.84 cm; 95% CI: 0.25 to 0.54; $P=0.009$). The indexed aortic diameters in DAo and in the mid-ascending

aorta did not change substantially, median difference 0.05 cm/m² (range -0.1 to 0.5 cm/m²; 95% CI: 0.01 to 0.22; $P=0.06$) for AAo, median difference -0.08 cm/m² (range -0.4 to 0.1 cm/m²; 95% CI: -0.12 to 0.01; $P=0.07$) for DAo. Values of the 10-year-old child are included in all analyses. Further baseline characteristics of the study population are displayed in *Table 1*. The three patients lost to follow-up are excluded in the column showing the data of 2008/2009.

Aortic distensibility and stiffness index

On AAo level, distensibility decreased by 25.6% when simultaneously aortic stiffness index increased by 23.6%. Values on DAo level behave in the same manner: distensibility decreased by 20.7% whereas aortic stiffness index increased by 22.4%. Median values and ranges of distensibility and stiffness index are presented in *Table 1*.

Flow visualization and WSS estimation

All patients with BAV showed right-handed, helical flow patterns in the mid-ascending aorta. One patient (6.7%) was classified as Grade 0, 3 patients (20.0%) as Grade 2 and 11 patients (73.3%) as Grade 3 (*Figure 2*). All patients with BAV type 2 (4, 100%), but only 7 patients with BAV type 1 (63.6%) were categorized as Grade 3. Helical flow patterns increased by at least one grading level after the 10-year follow-up period in five patients (33.3%). Comparison of flow patterns are illustrated in *Figure 3*, exemplary in two patients.

WSS values are displayed in *Table 1*. WSS_{axial} , WSS_{circ} and WSS_{mag} are lower in 2018/2019 at the MPA level as well as at the BCT level compared to 2008/2009 (*Figure 4*) even in the above-mentioned patients with an increment in flow grading as well as comparing values of our youngest patient, which was a child back in 2008 (WSS_{mag} decreased from 0.46 to 0.38 N/m² at MPA level and from 0.63 to 0.41 N/m² at BCT level). There were no relevant changes in all WSS directions on both aortic levels between BAV type 1 and BAV type 2. ROIs were placed at the identical levels as in the initial study, however we waived WSS measurement at the level of the aortic bulb due to weak resolution and therefore inadequate estimation of WSS since exact delineation of the aortic wall is crucial.

Intra- and inter-observer variability

Analysis showed good intra- and inter-observer variability:

Table 1 Study population characteristics

Characteristics	2008/2009 (n=15)		2018/2019 (n=15)		Median difference	95% CI of median difference	P value
	Median	Range	Median	Range			
Age (years)	24.5	10.1–43.6	34.0	19.8–54.3	9.5	9.8–10.3	0.004*
Height (cm)	173	138–192	175	160–191	2.0	–1.6 to 5.5	0.54
Weight (kg)	70.0	30.0–88.0	73.0	55.0–93.0	3.0	1.9–9.7	0.005*
BSA (m ²)	1.9	1.1–2.1	1.9	1.6–2.1	0	0.02–0.2	0.004*
BMI (kg/m ²)	22.8	15.8–28.1	24.4	20.8–30.4	1.6	0.4–2.8	0.02*
P _{sys} (mmHg)	110.5	92.0–128.0	112.0	111.0–130.0	1.5	–1.4 to 4.0	0.33
P _{dia} (mmHg)	62.0	44.0–83.0	64.5	53.0–87.0	2.5	0.3–5.0	0.04*
MAP (mmHg)	77.3	60.7–95.7	80.6	68.7–100.7	3.3	–0.1 to 4.5	0.07
V _{max} (m/s)	1.6	1.2–2.3	1.9	0.9–2.7	0.3	–5.0 to 52.8	0.03*
Regurgitation fraction (%)	1	0–6	2.5	0–13	1.5	–0.6 to 3.3	0.16
Absolute aortic diameter (cm)							
AAo	3.2	1.86–4.38	3.5	2.55–4.95	0.3	0.25–0.54	0.009*
DAo	1.8	1.38–2.23	1.8	1.30–2.24	0	–0.06 to 0.08	0.82
Indexed aortic diameter (cm/m ²)							
AAo	1.73	1.18–2.29	1.78	1.27–2.57	0.05	0.01–0.22	0.06
DAo	0.98	0.80–1.46	0.90	0.72–1.18	–0.08	–0.12 to 0.01	0.07
Distensibility (10 ^{–3} mmHg ^{–1})							
AAo	6.57	2.39–9.94	4.89	1.66–8.58	–1.68	–0.07 to 3.80	0.08
DAo	5.61	2.62–11.58	4.45	2.89–6.94	–1.16	–0.48 to 3.95	0.17
Stiffness index							
AAo	4.12	2.50–5.86	5.09	2.95–13.39	0.97	–4.83 to –0.13	0.02*
DAo	3.99	2.91–6.69	4.89	3.66–8.15	0.90	–3.02 to 0.33	0.17
WSS _{axial} (N/m ²)							
MPA level	0.45	0.29–0.74	0.28	0.22–0.51	–0.17	0.1–0.21	0.001*
BCT level	0.42	0.26–1.00	0.28	0.22–0.58	–0.14	0.08–0.21	0.003*
WSS _{circ} (N/m ²)							
MPA level	0.50	0.23–0.71	0.24	0.19–0.43	–0.16	0.15–0.29	0.001*
BCT level	0.48	0.22–1.04	0.27	0.22–0.61	–0.21	0.12–0.25	0.003*
WSS _{mag} (N/m ²)							
MPA level	0.75	0.40–1.15	0.43	0.34–0.75	–0.32	0.2–0.4	0.001*
BCT level	0.72	0.38–1.60	0.44	0.37–0.92	–0.27	0.16–0.36	0.002*

*, relevant changes after the follow-up period. BSA, body surface area; BMI, body mass index; P_{sys}, systolic blood pressure; P_{dia}, diastolic blood pressure; MAP, mean arterial pressure; V_{max}, maximal velocity through the aortic valve; AAo, (mid-) ascending aorta; DAo, descending aorta; BCT level, level before the branching of the brachiocephalic trunk; MPA level, level of bifurcation of the main pulmonary artery; WSS, wall shear stress; WSS_{axial}, axial WSS; WSS_{circ}, circumferential WSS; WSS_{mag}, magnitudinal WSS.

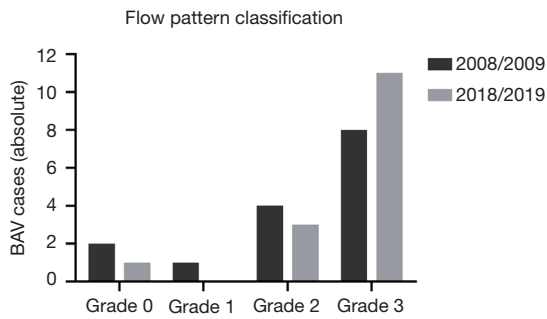


Figure 2 Bar chart of flow pattern classification (n=15). Grade 0: linear flow in the ascending aorta; Grade 1: helical flow <math><180^\circ</math>; Grade 2: helical flow of

mean values of WSS were 0.35 ± 0.10 and 0.34 ± 0.11 N/m^2 for the first and second measurement of one investigator ($r=0.97$) and 0.31 ± 0.08 N/m^2 ($r=0.68$) for the other investigator. Bland-Altman 95% limits of agreement were -0.03 to 0.05 N/m^2 and -0.04 to 0.11 N/m^2 .

Discussion

In this prospectively designed study, we could show that indexed diameter of the ascending and descending aorta in patients with BAV did not increase substantially over a follow-up period of ten years. Based on strict and specific exclusion criteria, a well-described patient cohort was

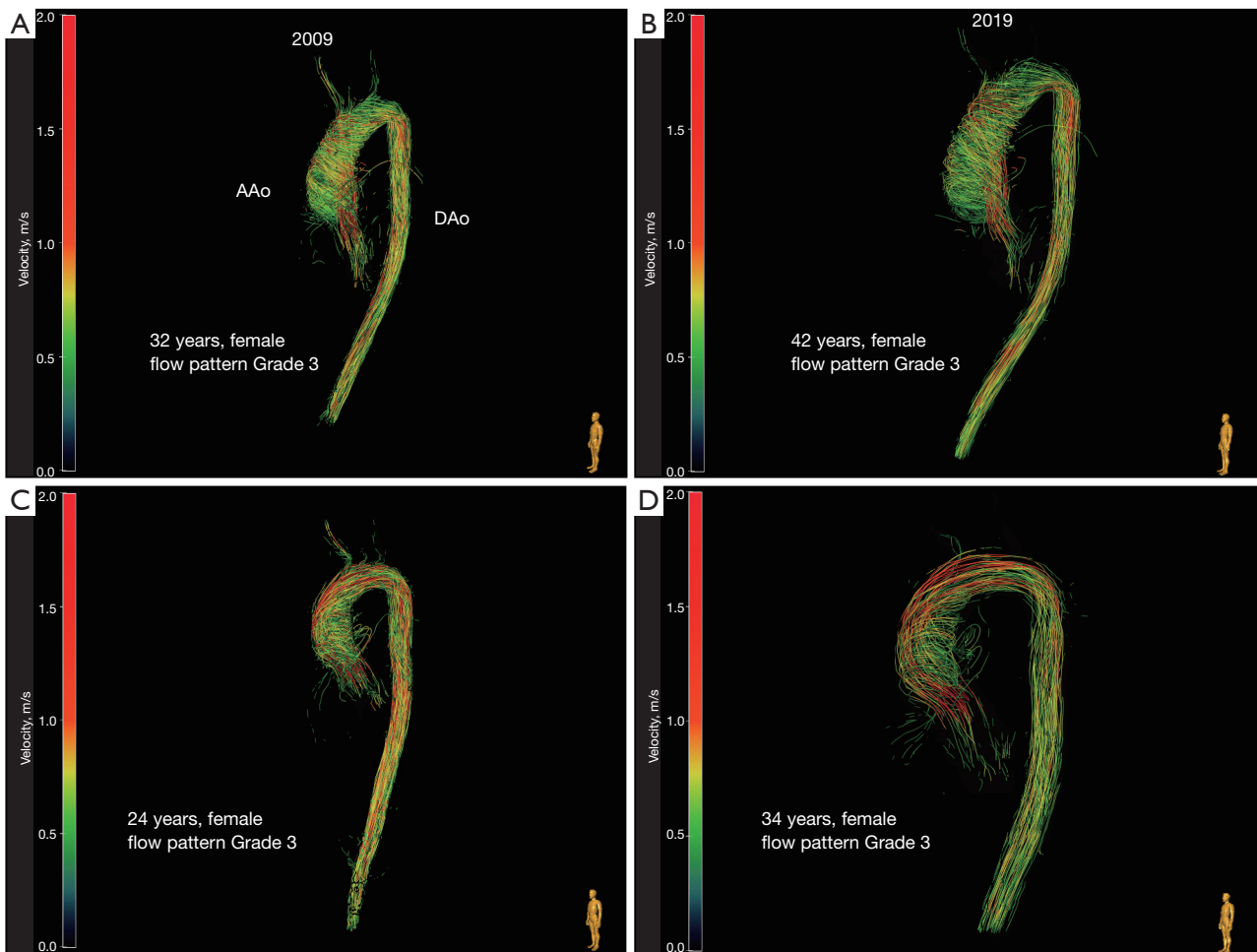


Figure 3 Pathline tracing of flow patterns in the ascending aorta in two patients. AAO, (mid-) ascending aorta; DAo, descending aorta.

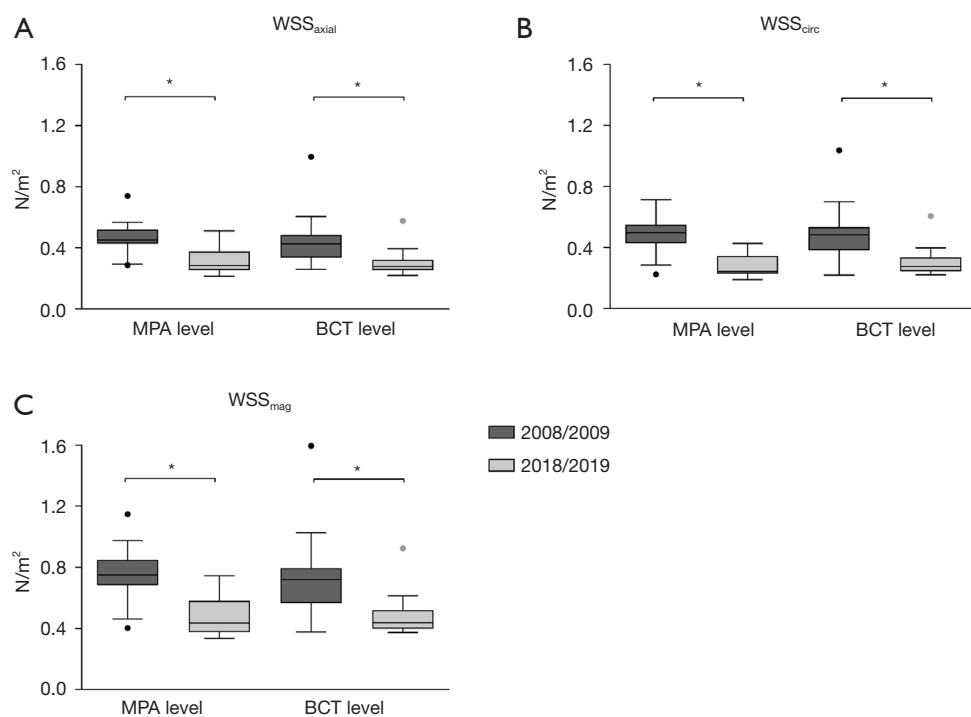


Figure 4 WSS: 10-year follow-up. Boxplot graphs (Tukey): (A) axial WSS, (B) circumferential WSS and (C) magnitudinal WSS measured at MPA level and BCT level. WSS_{axial} (95% CI: MPA level: 0.1 to 0.21, BCT level: 0.08 to 0.21; P value: MPA level: 0.001, BCT level: 0.003), WSS_{circ} (95% CI: MPA level: 0.15 to 0.29, BCT level: 0.12 to 0.25; P value: MPA level: 0.001, BCT level: 0.003) and WSS_{mag} (95% CI: MPA level: 0.2 to 0.4, BCT level: 0.16 to 0.36; P value: MPA level: 0.001, BCT level: 0.002). *, relevant changes after the follow-up period. WSS, wall shear stress; MPA, main pulmonary artery; BCT, brachiocephalic trunk.

formed back in 2008/2009. Fortunately, we were able to reevaluate the same, particular patient collective, still lacking any further cardiovascular disease than BAV. WSS was essentially lower in all directions and at all measured levels in the aorta. In accordance with age, aortic distensibility decreased and stiffness index increased over the given period.

Studies have shown that aortic diameters in patients with BAV are larger than in controls, even with a normally functioning valve (8). Surgical interventions in BAV disease can prevent these patients from complications and provide an excellent outcome in terms of survival (24), but aortic dilation after valve replacement is still present (25). Accordingly, an individual approach for risk stratification is required. In the pre-selected patient cohort of this study, absolute aortic diameter in AAO slightly increased. Whilst comparing aortic diameters, confounders were limited by applying a relation to physical conditions of the patients. After indexing the aortic diameters on BSA, the values did not change in a 10-year follow-up period

suggesting a potential benign long-term development and implementation of more conservative treatment strategies for the patients in our cohort study. Exact assessment of aortic size is under ongoing discussion in the literature, but though a height-based ratio seems to be sufficient, both correction for height as well as BSA improves prediction of complications (26,27). Semi-automatic assessment of aortic diameter may standardize measurements of aortic diameter (28).

Nevertheless, studies regarding outcome of BAV disease have revealed a higher prevalence for cardiac and vascular events compared to the general population (29). Besides aortic diameter, risk stratification includes severity of valvular dysfunction (30) or cardiovascular comorbidities such as CoA (31). The impact of flow alterations is also well demonstrated: helical flow patterns are present in BAV, especially in the mid-ascending aorta, including patients with concomitant aneurysm and aortic stenosis (AS) (32,33), creating “a higher friction of blood relative to the vessel wall with the consequence of increased WSS” (34). Several

previous studies have shown, comparing BAV patients to subjects with normal, tricuspid valves (TAV), that WSS is clearly increased in patients with BAV compared to TAV (6,11,35). Especially circumferential WSS and progression of helicity seem to have an impact on aortic growth (36,37). Heterogeneous distribution of WSS leads to different affections of the vessel wall, including elastic fiber thinning (38) as well as intima-media thickening and plaque induction in initiation of atherosclerosis (39). A few studies reported different results, that may be explained by varying characteristics of patient collective, measured ROI and investigated primary disease (40–42).

However, in due consideration of valvular function, a differentiation within the spectrum of BAV disease is necessary: follow-up data of non- or mild stenotic and/or regurgitant, isolated BAVs and concomitant WSS already revealed an almost asymptomatic, progression-free disease development (43), with stable WSS values in childhood (44), starting to decrease at middle age (45). This latter study supports the hypothesis that compared to TAV with dilation, BAV patients demonstrated WSS reduction as a compensatory mechanism to reduce elevated WSS forces by aortic remodeling. These studies support our findings: WSS substantially decreased in all spatial vectors and measured levels in the ascending aorta in our patient cohort. Even regarding values of the child aged only 10 years back in 2008/2009, we found a reduction of WSS. It is most remarkable, that changes in aortic diameter are not responsible for this drop of WSS. Regarding valvular dysfunction, Farag *et al.* found significantly elevated values of WSS, correlating with the severity of aortic valve stenosis (46). Despite peak velocity through the aortic valve was higher in our study and in 5 patients (33.3%) helical flow patterns increased by at least one grading level after the 10-year follow-up period, absolute values do not indicate a moderate or severe level of stenosis, making any major impact on WSS reduction unlikely. Although comparison of cohorts may be contestable due to various variations in patient characteristics, the paradox of results needs to be addressed. Because rotational flow was assessed using a subjective method and therefore may be subject to minor deviations in reevaluation, a more objective assessment of circulation may be focus in future work when better software tools measuring helical flow are available.

WSS reduction might be explained by slight alterations in hemodynamic flow patterns by the aging aorta: in the ascending as well as descending part, distensibility decreased and stiffness index increased both more than 20% after ten

years. In general, patients with BAV yet seem to exhibit altered elastic properties compared to normal controls, regardless of age (47). In addition, a positive correlation between age and stiffness suggests a continuous increase of stiffness over lifetime in BAV disease (48). Adjustment of distensibility to diameter may cause variation in changes of elastic properties and effects of valvular dysfunction have to be clarified (49,50), but our patients did not show any signs of disease progression. Numerical impairment of aortic elasticity may have led to changes in spatial and temporal distribution of helical flow. Slight alterations in flow direction, grade of rotation, angle to the vessel wall or intensity of helicity could have caused the decrease of WSS. It could serve as a marker for a benign long-term course, leading to prolonged intervals in serial reevaluation and a more conservative approach in therapy management.

Further studies are required for investigation of the impact of helical flow on WSS and the association between its severity and the development of aortopathy. Novel parameters may contribute to predict the outcome or even improve risk stratification: von Spiczak *et al.* described a quantitative analysis of vortical blood flow for visualization of pathological flow alterations (51), while Tiwari *et al.* successfully introduced so-called MRSD (maximal rate of systolic distension) and MRDR (maximal rate of diastolic recoil) for evaluation of biomechanical properties of the aorta (52). Future longitudinal studies should consider these parameters.

Limitations

Our study is a single-center study with a limited number of patients. Only adults, in 2008/2009 including one child, already pre-selected in 2008, especially concerning the absence of cardiac and vascular diseases further than BAV, were included [for information about initial recruitment refer to the previous study (6)]. Division into even smaller subgroups for comparison of different BAV morphologies is contestable, lacking statistical significance. Reevaluation of the exact same patient cohort as in 2008/2009 provides powerful long-term data, but results may not be interpreted as valid for the general population. Further longitudinal studies based on larger sample sizes are required.

Due to the study design, we were not aiming to gather histological specimens for the correlation of flow patterns and WSS with tissue alterations. Reevaluation of the reference group with TAV from the 2008/2009 study was also not included due to insufficient participation of former

evaluated TAV volunteers. Future work could take these aspects into account.

Even though we were able to use the same CMR sequence as in 2008/2009, software version of the scanner changed over ten years. As software version VB15 was used for the initial study, reevaluation was performed with the current version VD13. By approximating software parameters as accurate as possible, confounders were set to a minimum.

To avoid a measurement bias in post-processing, all data of 2008/2009 were reevaluated with the software MEVISFlow. However, feasibility of flow visualization and measurement of WSS has been proven (21,53) and is not affected by ongoing upgrade processes of the used software.

Identifying the vessel lumen border and positioning of ROIs has to be re-adjusted manually in each case and therefore may be subject to minor deviations in WSS estimation in future possible reevaluations. Systematical underestimation of WSS due to limited spatial resolution or partial volume effect in PC-CMR is an already well-known side effect (23). Newly developed approaches such as an automated segmentation-free method for computing WSS might increase accuracy and reproducibility of assessment of hemodynamic parameters (54).

Conclusions

After a ten years' follow-up period of patients with isolated BAV disease, indexed aortic diameters remained unchanged in the identical patient cohort. WSS was lower in all directions and at all measured aortic levels compared to values generated 10 years earlier. In accordance with a decreased aortic distensibility and an increased stiffness index, this might be explained by slight alterations in helical flow patterns by the aging aorta and due to remodeling. Possibly a drop in WSS in BAV could serve as a marker for a benign long-term course and implementation of more conservative treatment strategies in selected patients.

Acknowledgments

Funding: None.

Footnote

Provenance and Peer Review: This article was commissioned by the Guest Editors (Yskert von Kodolitsch, Harald Kaemmerer, Koichiro Niwa) for the series “Current

Management Aspects in Adult Congenital Heart Disease (ACHD): Part V” published in *Cardiovascular Diagnosis and Therapy*. The article has undergone external peer review.

Reporting Checklist: The authors have completed the TREND reporting checklist. Available at <https://cdt.amegroups.com/article/view/10.21037/cdt-22-477/rc>

Data Sharing Statement: Available at <https://cdt.amegroups.com/article/view/10.21037/cdt-22-477/dss>

Conflicts of Interest: All authors have completed the ICMJE uniform disclosure form (available at <https://cdt.amegroups.com/article/view/10.21037/cdt-22-477/coif>). The series “Current Management Aspects in Adult Congenital Heart Disease (ACHD): Part V” was commissioned by the editorial office without any funding or sponsorship. The authors have no other conflicts of interest to declare.

Ethical Statement: The authors are accountable for all aspects of the work in ensuring that questions related to the accuracy or integrity of any part of the work are appropriately investigated and resolved. The trial was conducted in accordance with the Declaration of Helsinki (as revised in 2013). The study was approved by the ethics committee of the Technical University of Munich (No. 29/18S). All patients gave written informed consent.

Open Access Statement: This is an Open Access article distributed in accordance with the Creative Commons Attribution-NonCommercial-NoDerivs 4.0 International License (CC BY-NC-ND 4.0), which permits the non-commercial replication and distribution of the article with the strict proviso that no changes or edits are made and the original work is properly cited (including links to both the formal publication through the relevant DOI and the license). See: <https://creativecommons.org/licenses/by-nc-nd/4.0/>.

References

1. Fedak PW, Verma S, David TE, et al. Clinical and pathophysiological implications of a bicuspid aortic valve. *Circulation* 2002;106:900-4.
2. Sillesen AS, Vøgg O, Pihl C, et al. Prevalence of Bicuspid Aortic Valve and Associated Aortopathy in Newborns in Copenhagen, Denmark. *JAMA* 2021;325:561-7.
3. Braverman AC, Güven H, Beardslee MA, et al. The bicuspid aortic valve. *Curr Probl Cardiol* 2005;30:470-522.

4. Schaefer BM, Lewin MB, Stout KK, et al. The bicuspid aortic valve: an integrated phenotypic classification of leaflet morphology and aortic root shape. *Heart* 2008;94:1634-8.
5. Ward C. Clinical significance of the bicuspid aortic valve. *Heart* 2000;83:81-5.
6. Meierhofer C, Schneider EP, Lyko C, et al. Wall shear stress and flow patterns in the ascending aorta in patients with bicuspid aortic valves differ significantly from tricuspid aortic valves: a prospective study. *Eur Heart J Cardiovasc Imaging* 2013;14:797-804.
7. Michelena HI, Khanna AD, Mahoney D, et al. Incidence of aortic complications in patients with bicuspid aortic valves. *JAMA* 2011;306:1104-12.
8. Nkomo VT, Enriquez-Sarano M, Ammash NM, et al. Bicuspid aortic valve associated with aortic dilatation: a community-based study. *Arterioscler Thromb Vasc Biol* 2003;23:351-6.
9. McKusick VA. Association of congenital bicuspid aortic valve and Erdheim's cystic medial necrosis. *Lancet* 1972;1:1026-7.
10. Girdauskas E, Borger MA, Secknus MA, et al. Is aortopathy in bicuspid aortic valve disease a congenital defect or a result of abnormal hemodynamics? A critical reappraisal of a one-sided argument. *Eur J Cardiothorac Surg* 2011;39:809-14.
11. Barker AJ, Lanning C, Shandas R. Quantification of hemodynamic wall shear stress in patients with bicuspid aortic valve using phase-contrast MRI. *Ann Biomed Eng* 2010;38:788-800.
12. Santarpia G, Scognamiglio G, Di Salvo G, et al. Aortic and left ventricular remodeling in patients with bicuspid aortic valve without significant valvular dysfunction: a prospective study. *Int J Cardiol* 2012;158:347-52.
13. Writing Committee Members, Otto CM, Nishimura RA, et al. 2020 ACC/AHA Guideline for the Management of Patients With Valvular Heart Disease: A Report of the American College of Cardiology/American Heart Association Joint Committee on Clinical Practice Guidelines. *J Am Coll Cardiol* 2021;77:e25-e197.
14. Stankovic Z, Allen BD, Garcia J, et al. 4D flow imaging with MRI. *Cardiovasc Diagn Ther* 2014;4:173-92.
15. Markl M, Frydrychowicz A, Kozierke S, et al. 4D flow MRI. *J Magn Reson Imaging* 2012;36:1015-36.
16. Frydrychowicz A, Stalder AF, Russe MF, et al. Three-dimensional analysis of segmental wall shear stress in the aorta by flow-sensitive four-dimensional-MRI. *J Magn Reson Imaging* 2009;30:77-84.
17. Markl M, Draney MT, Hope MD, et al. Time-resolved 3-dimensional velocity mapping in the thoracic aorta: visualization of 3-directional blood flow patterns in healthy volunteers and patients. *J Comput Assist Tomogr* 2004;28:459-68.
18. Groenink M, de Roos A, Mulder BJ, et al. Changes in aortic distensibility and pulse wave velocity assessed with magnetic resonance imaging following beta-blocker therapy in the Marfan syndrome. *Am J Cardiol* 1998;82:203-8.
19. Nistri S, Grande-Allen J, Noale M, et al. Aortic elasticity and size in bicuspid aortic valve syndrome. *Eur Heart J* 2008;29:472-9.
20. Walker PG, Cranney GB, Scheidegger MB, et al. Semiautomated method for noise reduction and background phase error correction in MR phase velocity data. *J Magn Reson Imaging* 1993;3:521-30.
21. Zimmermann J, Demedts D, Mirzaee H, et al. Wall shear stress estimation in the aorta: Impact of wall motion, spatiotemporal resolution, and phase noise. *J Magn Reson Imaging* 2018. [Epub ahead of print]. doi: 10.1002/jmri.26007.
22. Napel S, Lee DH, Frayne R, et al. Visualizing three-dimensional flow with simulated streamlines and three-dimensional phase-contrast MR imaging. *J Magn Reson Imaging* 1992;2:143-53.
23. Stalder AF, Russe MF, Frydrychowicz A, et al. Quantitative 2D and 3D phase contrast MRI: optimized analysis of blood flow and vessel wall parameters. *Magn Reson Med* 2008;60:1218-31.
24. Badiu CC, Eichinger W, Bleiziffer S, et al. Should root replacement with aortic valve-sparing be offered to patients with bicuspid valves or severe aortic regurgitation? *Eur J Cardiothorac Surg* 2010;38:515-22.
25. Hörer J, Hanke T, Stierle U, et al. Neoaortic root diameters and aortic regurgitation in children after the Ross operation. *Ann Thorac Surg* 2009;88:594-600; discussion 600.
26. Zafar MA, Li Y, Rizzo JA, et al. Height alone, rather than body surface area, suffices for risk estimation in ascending aortic aneurysm. *J Thorac Cardiovasc Surg* 2018;155:1938-50.
27. Elefteriades JA, Mukherjee SK, Mojiabian H. Discrepancies in Measurement of the Thoracic Aorta: JACC Review Topic of the Week. *J Am Coll Cardiol* 2020;76:201-17.
28. Dux-Santoy L, Rodríguez-Palomares JF, Teixidó-Turà G, et al. Registration-based semi-automatic assessment of aortic diameter growth rate from contrast-enhanced

- computed tomography outperforms manual quantification. *Eur Radiol* 2022;32:1997-2009.
29. Michelena HI, Desjardins VA, Avierinos JF, et al. Natural history of asymptomatic patients with normally functioning or minimally dysfunctional bicuspid aortic valve in the community. *Circulation* 2008;117:2776-84.
 30. Geiger J, Rahsepar AA, Suwa K, et al. 4D flow MRI, cardiac function, and T(1) -mapping: Association of valve-mediated changes in aortic hemodynamics with left ventricular remodeling. *J Magn Reson Imaging* 2018;48:121-31.
 31. Sinning C, Zengin E, Kozlik-Feldmann R, et al. Bicuspid aortic valve and aortic coarctation in congenital heart disease-important aspects for treatment with focus on aortic vasculopathy. *Cardiovasc Diagn Ther* 2018;8:780-8.
 32. Bissell MM, Hess AT, Biasioli L, et al. Aortic dilation in bicuspid aortic valve disease: flow pattern is a major contributor and differs with valve fusion type. *Circ Cardiovasc Imaging* 2013;6:499-507.
 33. Shan Y, Li J, Wang Y, et al. Aortic stenosis exacerbates flow aberrations related to the bicuspid aortic valve fusion pattern and the aortopathy phenotype. *Eur J Cardiothorac Surg* 2019;55:534-42.
 34. Lorenz R, Bock J, Barker AJ, et al. 4D flow magnetic resonance imaging in bicuspid aortic valve disease demonstrates altered distribution of aortic blood flow helicity. *Magn Reson Med* 2014;71:1542-53.
 35. Soulat G, Scott MB, Allen BD, et al. Association of Regional Wall Shear Stress and Progressive Ascending Aorta Dilation in Bicuspid Aortic Valve. *JACC Cardiovasc Imaging* 2022;15:33-42.
 36. Minderhoud SCS, Roos-Hesselink JW, Chelu RG, et al. Wall shear stress angle is associated with aortic growth in bicuspid aortic valve patients. *Eur Heart J Cardiovasc Imaging* 2022;23:1680-9.
 37. Guala A, Dux-Santoy L, Teixido-Tura G, et al. Wall Shear Stress Predicts Aortic Dilation in Patients With Bicuspid Aortic Valve. *JACC Cardiovasc Imaging* 2022;15:46-56.
 38. Bollache E, Guzzardi DG, Sattari S, et al. Aortic valve-mediated wall shear stress is heterogeneous and predicts regional aortic elastic fiber thinning in bicuspid aortic valve-associated aortopathy. *J Thorac Cardiovasc Surg* 2018;156:2112-2120.e2.
 39. Cheng C, Tempel D, van Haperen R, et al. Atherosclerotic lesion size and vulnerability are determined by patterns of fluid shear stress. *Circulation* 2006;113:2744-53.
 40. Allen BD, van Ooij P, Barker AJ, et al. Thoracic aorta 3D hemodynamics in pediatric and young adult patients with bicuspid aortic valve. *J Magn Reson Imaging* 2015;42:954-63.
 41. Boussel L, Rayz V, McCulloch C, et al. Aneurysm growth occurs at region of low wall shear stress: patient-specific correlation of hemodynamics and growth in a longitudinal study. *Stroke* 2008;39:2997-3002.
 42. Geiger J, Arnold R, Herzer L, et al. Aortic wall shear stress in Marfan syndrome. *Magn Reson Med* 2013;70:1137-44.
 43. Mills P, Leech G, Davies M, et al. The natural history of a non-stenotic bicuspid aortic valve. *Br Heart J* 1978;40:951-7.
 44. Rose MJ, Rigsby CK, Berhane H, et al. 4-D flow MRI aortic 3-D hemodynamics and wall shear stress remain stable over short-term follow-up in pediatric and young adult patients with bicuspid aortic valve. *Pediatr Radiol* 2019;49:57-67.
 45. Rahman O, Scott M, Bollache E, et al. Interval changes in aortic peak velocity and wall shear stress in patients with bicuspid aortic valve disease. *Int J Cardiovasc Imaging* 2019;35:1925-34.
 46. Farag ES, van Ooij P, Planken RN, et al. Aortic valve stenosis and aortic diameters determine the extent of increased wall shear stress in bicuspid aortic valve disease. *J Magn Reson Imaging* 2018;48:522-30.
 47. Goudot G, Mirault T, Bruneval P, et al. Aortic Wall Elastic Properties in Case of Bicuspid Aortic Valve. *Front Physiol* 2019;10:299.
 48. de Wit A, Vis K, Jeremy RW. Aortic stiffness in heritable aortopathies: relationship to aneurysm growth rate. *Heart Lung Circ* 2013;22:3-11.
 49. Guala A, Rodriguez-Palomares J, Dux-Santoy L, et al. Influence of Aortic Dilation on the Regional Aortic Stiffness of Bicuspid Aortic Valve Assessed by 4-Dimensional Flow Cardiac Magnetic Resonance: Comparison With Marfan Syndrome and Degenerative Aortic Aneurysm. *JACC Cardiovasc Imaging* 2019;12:1020-9.
 50. Singh A, Horsfield MA, Bekele S, et al. Aortic stiffness in aortic stenosis assessed by cardiovascular MRI: a comparison between bicuspid and tricuspid valves. *Eur Radiol* 2019;29:2340-9.
 51. von Spiczak J, Crelier G, Giese D, et al. Quantitative Analysis of Vortical Blood Flow in the Thoracic Aorta Using 4D Phase Contrast MRI. *PLoS One* 2015;10:e0139025.
 52. Tiwari KK, Bevilacqua S, Aquaro GD, et al. Functional Magnetic Resonance Imaging in the Evaluation of the Elastic Properties of Ascending Aortic Aneurysm. *Braz J*

- Cardiovasc Surg 2019;34:451-7.
53. Rizk J, Latus H, Shehu N, et al. Elevated diastolic wall shear stress in regurgitant semilunar valvular lesions. *J Magn Reson Imaging* 2019;50:763-70.
54. Masutani EM, Contijoch F, Kyubwa E, et al. Volumetric segmentation-free method for rapid visualization of vascular wall shear stress using 4D flow MRI. *Magn Reson Med* 2018;80:748-55.

Cite this article as: Hanigk M, Burgstaller E, Latus H, Shehu N, Zimmermann J, Martinoff S, Hennemuth A, Ewert P, Stern H, Meierhofer C. Aortic wall shear stress in bicuspid aortic valve disease—10-year follow-up. *Cardiovasc Diagn Ther* 2023;13(1):38-50. doi: 10.21037/cdt-22-477